Fourth-generation charged leptons and neutrinos via Z^0

H. Baer
CERN, CH-1211, Genève 23, Switzerland

V. Barger
Physics Department, University of Wisconsin, Madison, Wisconsin 53706

R. J. N. Phillips
Rutherford Appleton Laboratory, Chilton, Oxon, England
(Received 15 March 1985)

The decays $Z^0\to L\bar{L}$ and $Z^0\to\nu_4\bar{\nu}_4$ are promising sources of a possible fourth-generation charged lepton and its neutrino, both of which may be heavy. We give expressions for the rates and differential distributions, including production and decay correlations, for e^+e^- and $p\bar{p}$ production via real or virtual Z^0. We evaluate the different leptonic and hadronic signatures in e^+e^- collisions and present rates for dileptons from $L\bar{L}$ production in $p\bar{p}$ collisions.

I. INTRODUCTION

With the energies now available or soon to be available at $p\bar{p}$ and e^+e^- colliders, it is feasible to search for possible fourth-generation quarks and leptons.[1–8] For the case of a charged heavy lepton L, it is feasible to detect L and measure its mass through W production with $W\to L\nu$ decay at $p\bar{p}$ colliders.[2] In the present paper we consider complementary ways to detect L leptons, via real or virtual Z^0 production with $Z^0\to L\bar{L}$ decay, which offer interesting new signatures that can be pursued primarily at e^+e^- colliders. We give cross-section expressions including full production and decay correlations, for L leptonic and hadronic decays (see also Ref. 9). Our general considerations apply equally to $Z^0\to\tau\bar{\tau}$ which can serve as a calibration. We also discuss heavy fourth-generation neutrino production via $Z^0\to\nu_4\bar{\nu}_4$, with charged-current ν_4 decay, for which the same matrix elements can be adapted.

It is already known that the L mass is greater than 22 GeV from e^+e^- collider experiments.[10] The decay rates in the channels $L\to e\nu\nu$, $\mu\nu\nu$, $\tau\nu\nu$, $\bar{u}d\nu$, $\bar{c}s\nu$ are in the approximate ratios 1:1:1:3:3, hence the two primary classes of decays $L\to l+\not{p}_T$ ($l=e$ or μ and $\not{p}_T=$missing energy-momentum of neutrinos) and $L\to\bar{q}_1q_2+\not{p}_T$ ($q_1,q_2=$quark jets) are in the ratio 12:33. The signatures for $Z^0\to L\bar{L}$ fall in the following three distinctive categories, in the approximate proportions 6:33:45.

(i) $l_1\bar{l}_2+\not{p}_T$, a pair of opposite-sign leptons (which may have different flavors) along with missing energy-momentum from neutrinos.

(ii) $lq_1\bar{q}_2+\not{p}_T$, a single charged lepton with up to two hadronic jets plus missing energy-momentum.

(iii) $q_1\bar{q}_2q_3\bar{q}_4+\not{p}_T$, up to four jets.

In the case of a c-quark jet, semileptonic charm decay can give an additional lepton accompanied by hadrons. It is naturally understood that the hadronic jets arising from individual quarks may sometimes overlap to form broader jets; in the case of τ decay the $q_1\bar{q}_2$ give a single narrow hadronic jet.

In the following sections we give formulas for the differential distributions of leptons and quarks resulting from $L\bar{L}$ production via Z^0 and γ^* intermediate states, and explain how these formulas can also be applied to $\nu_4\bar{\nu}_4$ production.

II. PRODUCTION OF $L\bar{L}$ IN $p\bar{p}$ AND e^+e^- COLLIDERS

We consider the production of pairs of heavy charged leptons through the subprocesses

$$f\bar{f}\to Z,\gamma^*\to L\bar{L}\ , \tag{1}$$

where f stands for the electron or any of the light quarks u, d, or s in a hadron beam. The amplitude for this process is

$$\mathcal{M}=\frac{e^2Q_fQ_L}{\hat{s}}\bar{v}(\bar{f})\gamma_\mu u(f)\bar{u}(L)\gamma^\mu v(\bar{L})+\frac{8G_F{M_Z}^2}{\sqrt{2}}D_Z(\hat{s})\bar{v}(\bar{f})\gamma_\mu\times(g_V^f-g_A^f\gamma_5)u(f)\bar{u}(L)\gamma^\mu(g_V^L-g_A^L\gamma_5)v(\bar{L})\ . \tag{2}$$

Particle labels are used to denote four-momenta, $\hat{s}=(f+\bar{f})^2$ is the subprocess c.m. energy squared, D_Z is the propagator factor

$$D_Z(\hat{s})=(\hat{s}-{M_Z}^2+iM_Z\Gamma_Z)^{-1}\ ,$$

and the Z couplings to fermions in the standard model are

$$g_V^i=\tfrac{1}{2}(T_3^i-2Q^i x_W),\quad g_A^i=\tfrac{1}{2}T_3^i\ .$$

Here, T_3^i and Q^i are the third component of weak isospin, and the electric charge of the associated quark or lepton i. The total cross section is given by

$$\sigma=\frac{\beta\hat{s}}{12\pi}[C_1(1-m_L{}^2/\hat{s})+3C_2 m_L{}^2/\hat{s}]\ , \tag{3}$$

where

$$\beta=(1-4m_L{}^2/\hat{s})^{1/2}\ , \tag{4}$$

$$C_1=|G_{VV}|^2+|G_{AA}|^2+|G_{AV}|^2+|G_{VA}|^2\ , \tag{5}$$

$$C_2=|G_{VV}|^2+|G_{AV}|^2-|G_{AA}|^2-|G_{VA}|^2\ , \tag{6}$$

$$G_{VV}=\frac{e^2Q_fQ_L}{\hat{s}}+\frac{8G_FM_Z{}^2D_Z(\hat{s})}{\sqrt{2}}g_V^f g_V^L\ , \tag{7}$$

$$G_{AA}=\frac{8G_FM_Z{}^2D_Z(\hat{s})}{\sqrt{2}}g_A^f g_A^L\ , \tag{8}$$

$$G_{AV}=-\frac{8G_FM_Z{}^2D_Z(\hat{s})}{\sqrt{2}}g_A^f g_V^L\ , \tag{9}$$

$$G_{VA}=-\frac{8G_FM_Z{}^2D_Z(\hat{s})}{\sqrt{2}}g_V^f g_A^L\ . \tag{10}$$

This cross-section formula reduces to the result of Ref. 6 for the case of $e^+e^-\to L\bar{L}$.

Total cross sections for $L\bar{L}$ production in $p\bar{p}$ colliders have been presented in Ref. 1 for two sets of parton distributions, at c.m. energies of 0.54, 2, and 20 TeV. The cross section at 0.54 TeV varies from 20–50 pb for a heavy lepton of mass 20–45 GeV. Branching fractions to different decay modes and experimental acceptance cuts reduce this signal to the 1 pb level, making detection of $L\bar{L}$ from Z^0 decay difficult at the CERN collider. The cross section for $L\bar{L}$ production at a 2-TeV collider is an order of magnitude higher for the same range in m_L.

An e^+e^- collider operating at Z^0 resonance could be a prolific source of heavy-lepton pairs, provided that $m_L<m_Z/2$. Figure 1 shows a plot of the ratio

$$R=\frac{\sigma(e^+e^-\to L^+L^-)}{\sigma(e^+e^-\to\mu^+\mu^-)} \tag{11}$$

for different choices of mass of the heavy lepton L, versus the center-of-mass energy $\sqrt{s}$. The dip in the curves at the Z^0 resonance is caused by the mass sensitive term involving C_2 in Eq. (3). At the Z^0 resonance, the γ^* and Z^0 production mechanisms decouple, the interference term going to zero, and the Z^0 contribution dominates. The production rate of $L\bar{L}$ pairs for e^+e^- machines operating at the Z^0 resonance is very sensitive to m_L, and can indeed be used to determine m_L if the $L\bar{L}$ events are readily distinguishable from background. An independent measurement of m_L can be made from the sharp rise in event rate as the c.m. energy rises above $L\bar{L}$ production threshold.

The preceding formulation applies equally to the production of Dirac neutrinos via $f\bar{f}\to Z^0\to\nu_4\bar{\nu}_4$, setting $Q_L=O$ and $T_3^L=+\frac{1}{2}$ for $L=\nu_4$. For the case of a Majorana neutrino, $g_V^L=0$, $g_A^L=T_3^L$, and the right-hand side of Eq. (3) must be divided by 2 for identical-particle phase space. Figure 2 shows the cross-section ratio $\sigma(e^+e^-\to\nu_4\bar{\nu}_4)/\sigma(e^+e^-\to\mu^+\mu^-)$ versus $\sqrt{s}$ for several values of the ν_4 mass.

An unexplained event[11] observed at DESY PETRA by the CELLO collaboration at $\sqrt{s}=43.7$ GeV has the possible interpretation of $e^+e^-\to\nu_4\bar{\nu}_4$ production with $\nu_4\to\mu+$jet decays (see also Ref. 12). The event contains μ^+ and μ^- with two jets that are approximately back-to-back with the muons. The invariant masses of the μ plus opposite jet systems are about 20 GeV, which would imply a ν_4 mass of that magnitude. Figure 3 shows the expected $\nu_4\bar{\nu}_4$ cross section at $\sqrt{s}=43.7$ versus ν_4 mass; the cross sections are suppressed by the threshold kinematics, especially for the Majorana case because the axial-vector coupling is P wave. The luminosity of the data taken near this energy is 3.9 pb^{-1}; for a ν_4 mass of 20 GeV about 1.3 events are expected for a Dirac neutrino as compared to 0.2 events for a Majorana neutrino.

III. RATES AND SIGNATURES FOR $Z^0\to L\bar{L}$ CHANNELS

Calculation of distributions of detectable final-state particles from $Z^0\to L\bar{L}$ (or $\nu_4\bar{\nu}_4$) requires knowledge of the matrix element squared of production and decay, retaining the intermediate heavy-lepton helicity information, as illustrated in Fig. 4 for leptonic $L\bar{L}$ decays. This calculation is long but straightforward, and details are given in the Appendix. The results are general, and can be adapted for production through γ^* or Z^0, for $L\bar{L}$ or $\nu_4\bar{\nu}_4$ production, and for both leptonic and semileptonic decays. In the following subsections we discuss the numerical rates and distributions for different channels.

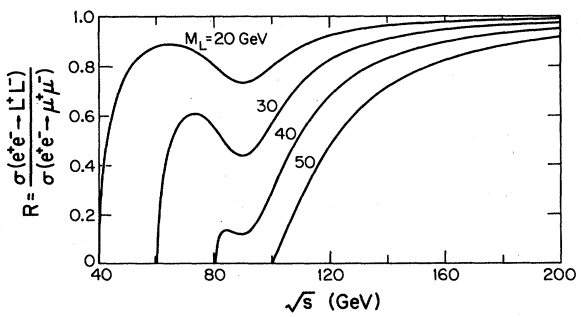

FIG. 1. Ratio of $L\bar{L}$ to $\mu\bar{\mu}$ events for various L masses and c.m. energies in e^+e^- collisions.

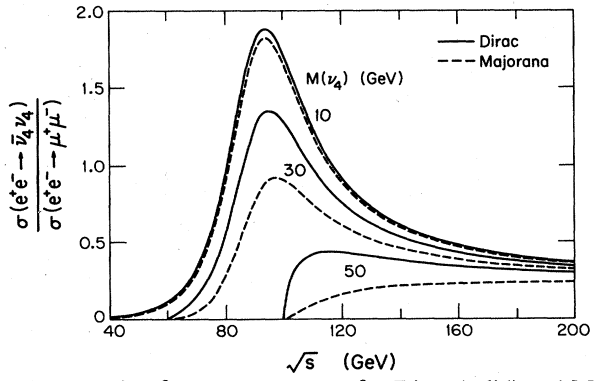

FIG. 2. Ratio of $\nu_4\bar{\nu}_4$ to $\mu\bar{\mu}$ events for Dirac (solid) and Majorana (dashed) neutrinos as a function of c.m. energy in e^+e^- collisions.

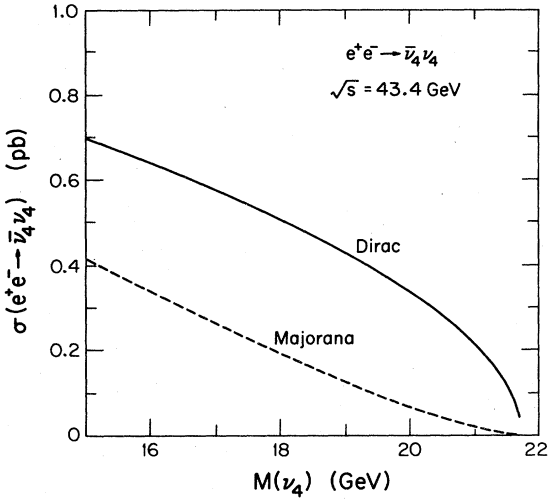

FIG. 3. Expected cross sections for $e^+e^- \to Z \to \nu_4\bar{\nu}_4$ for Dirac (solid) and Majorana (dashed) neutrinos as a function of neutrino mass at $\sqrt{s} = 43.4$ GeV.

A. Dilepton signals

$p\bar{p}$ collisions. Table I gives total cross sections for dilepton production in $p\bar{p}$ collisions via heavy leptons from Z^0 decay. Our results for the CERN collider energy $\sqrt{s} = 630$ GeV include full experimental cuts and momentum resolution smearing for the UA1 detector, as defined in Ref. 13. We include an empirical QCD-motivated factor of $K = 2$, and convolute the subprocess with Duke-Owens I parton distributions.[14] These signals are at the fraction of a pb level, and likely too small ever to be seen at CERN.

Also included in Table I are results for the Fermilab collider at $\sqrt{s} = 2$ TeV. These calculations include no cuts or resolution smearing. Cross sections at the Fermilab Tevatron energy are about an order of magnitude higher than those at the CERN energy. Owing to the smallness of the $p\bar{p}$ cross sections, we do not present the corresponding lepton distributions.

e^+e^- collisions. An e^+e^- machine operating at Z^0 resonance could be a copious source of heavy leptons.

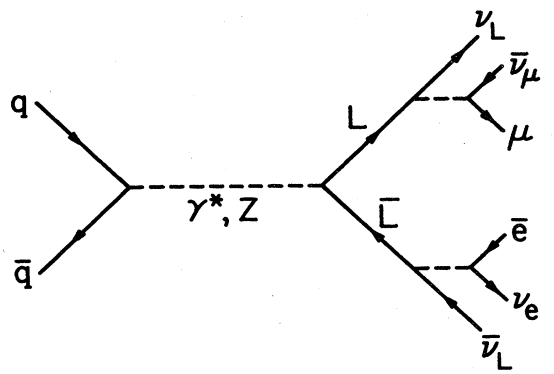

FIG. 4. Feynman diagram illustrating $Z^0 \to L\bar{L}$ production of fourth-generation charged leptons, and their subsequent semileptonic decays.

TABLE I. Total expected cross sections for the production and decay of heavy leptons via Z^0 decay at $p\bar{p}$ colliders. The results for the CERN energy of $\sqrt{s} = 630$ GeV include experimental cuts and measurement resolution in accord with the UA1 detector (see Ref. 13). The results for the Tevatron energy $\sqrt{s} = 2000$ GeV include no cuts or resolution. The results for $p\bar{p} \to Z \to L\bar{L} \to e\mu + \not{p}_T$ are expected to be $\sigma_{e\mu} = \sigma_{ee} + \sigma_{\mu\mu}$. The cross sections include a factor $K = 2$.

Process	$\sqrt{s}$ (GeV)	m_L (GeV)	σ_{ee} (pb)	$\sigma_{\mu\mu}$ (pb)
$p\bar{p} \to Z \to \tau\bar{\tau} \to l^+l^- + \not{p}_T$	630	1.78	0.55	1.32
$p\bar{p} \to Z \to L\bar{L} \to l^+l^- + \not{p}_T$	630	25	0.15	0.46
$p\bar{p} \to Z \to L\bar{L} \to l^+l^- + \not{p}_T$	630	40	0.07	0.15
$p\bar{p} \to Z \to \tau\bar{\tau} \to l^+l^- + \not{p}_T$	2000	1.78	7.16	7.16
$p\bar{p} \to Z \to L\bar{L} \to l^+l^- + \not{p}_T$	2000	25	2.14	2.14
$p\bar{p} \to Z \to L\bar{L} \to l^+l^- + \not{p}_T$	2000	40	0.67	0.67

The reaction $Z^0 \to L\bar{L}$, with each L decaying leptonically, should provide a very clean signal. The expected rate of the leptonic channels into e and μ is about 5% of the total $L\bar{L}$ signal. The ee, $\mu\mu$, $e\mu$ opposite-sign dileptons would occur in the ratio of 1:1:2. There would be no accompanying hadronic activity. The trigger leptons would be acollinear, distributed in dilepton opening angle $\Delta\theta_{ll}$ according to Fig. 5. The peak in the opening angle distribution between leptons in $L\bar{L}$ production depends on the L mass. Dileptons from the background process $Z \to \tau\bar{\tau}$

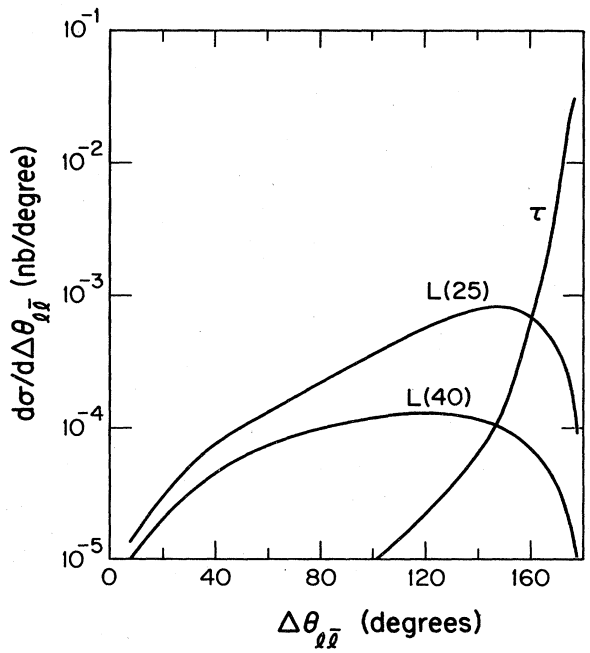

FIG. 5. Distribution in dilepton opening angle from the reaction $e^+e^- \to Z^0 \to L\bar{L}$, where each L decays leptonically at c.m. energy $\sqrt{s} = 94$ GeV $= m_Z$. Also shown is the background contribution from $Z^0 \to \tau\bar{\tau}$.

should be nearly back to back. Figure 6 shows the distribution in the component of the lepton distribution normal to the plane containing the beam and the other lepton, obtained with the τ, $L(25)$, and $L(40)$.

B. l-jet (s) signal

$p\bar{p}$ collisions. When one L decays leptonically, and one hadronically, the signal is an isolated electron or muon, one or two jets (depending on the jet-counting algorithm) and missing transverse momentum. Cross sections for this signal are about a factor of 6 larger than the dilepton signal, due to larger branching fractions. Detection of such events will be hampered by large backgrounds from heavy quark production, and by the $Z\to\tau\bar{\tau}$ contribution from events where the Z is accompanied by substantial jet energy.

e^+e^- collisions. Prospects for detecting lepton-plus-jet events from $Z\to L\bar{L}$ are much better at e^+e^- colliders because of rate, improved jet resolution, and greatly reduced background problems. The decay $L\to\nu_L q\bar{Q}$ produces two narrow jets. Figure 7 gives the opening angle between these two jets for heavy-lepton masses of 25 and 40 GeV. The invariant mass of these two jets can be used for L mass determination, as the dijet mass is always bounded by m_L. Figure 8 compares the m_{JJ} distributions obtained with the τ, $m_L(25)$, and $m_L(40$ GeV), for an e^+e^- machine operating on the Z resonance.

A background process is $Z\to Q\bar{Q}$ where $Q=b$ or c, with one Q decaying semileptonically. Here the trigger lepton will be accompanied by hadronic debris. Lepton-isolation cuts can be used to suppress this background.

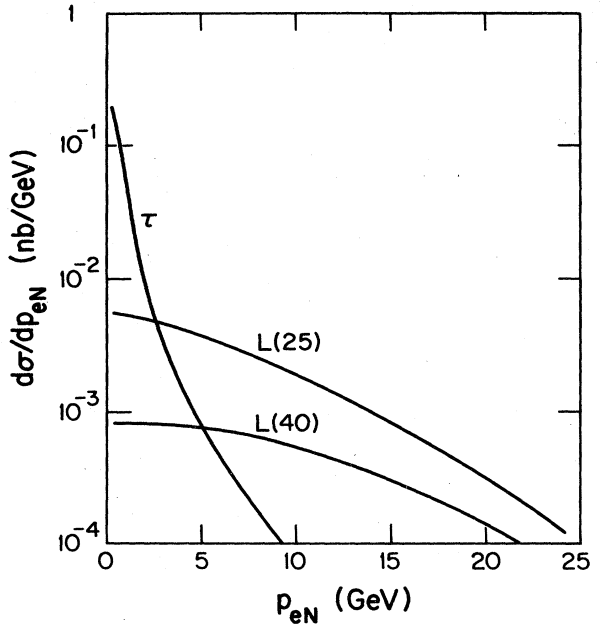

FIG. 6. The component of lepton momentum normal to the plane containing the beam and the other lepton in the reaction $e^+e^-\to Z^0\to L\bar{L}\to l^+l^-+\not{p}_T$, for an e^+e^- machine operating at Z^0 resonance.

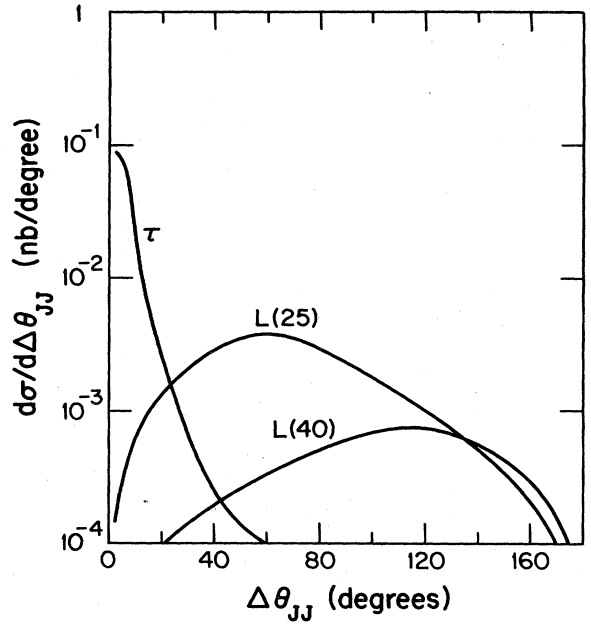

FIG. 7. The jet-jet opening angle for jets produced in the reaction $e^+e^-\to Z^0\to L\bar{L}\to l\bar{q}Q+\not{p}_T$, for e^+e^- annihilation at Z^0 resonance.

C. Four-jet, missing-energy signal

The last charged-heavy-lepton signal to be considered is where each L of the $L\bar{L}$ pair decays hadronically, which occurs 44% of the time. In this case there will be up to four jets distributed in 4π sr, accompanied by missing energy. In general, correlations between the different jets will be hard to determine.

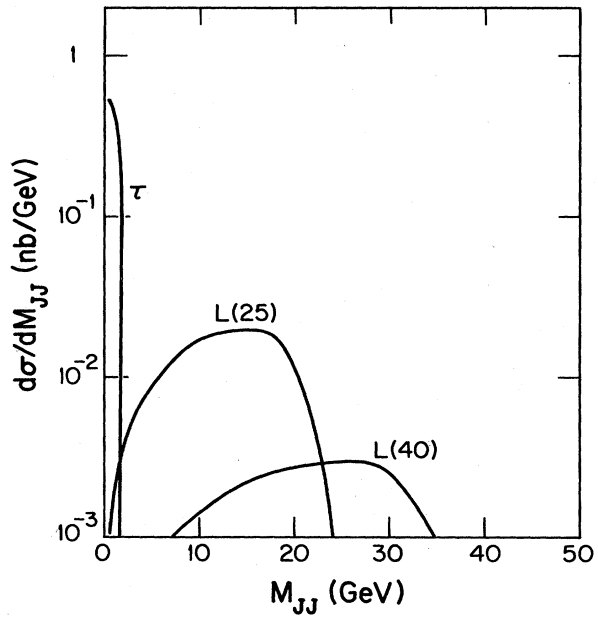

FIG. 8. The jet-jet invariant mass from the two-quark jets in the reaction $e^+e^-\to Z^0\to L\bar{L}\to l\bar{q}Q+\not{p}_T$, at Z^0 resonance.

D. l–l–two-jet events from $Z^0 \to \nu_4 \bar{\nu}_4$

The observation of an event with two muons and two jets by the CELLO collaboration[11] could possibly be a signal for fourth-generation neutrinos produced via $e^+e^- \to Z^0 \to \nu_4\bar{\nu}_4$, each ν_4 decaying to a muon plus a jet. The cross section for ν_4 production at the c.m. energy $\sqrt{s} = 43.4$ GeV of the CELLO event has been given in Fig. 3; the rate also depends on the branching fraction. The predicted energy distribution of muons and jets from this process are shown in Fig. 9 for a ν_4 mass of 20 GeV, along with the energies of the particles in the CELLO event. The muon energy distribution peaks around 6 GeV, compared to 15 GeV for the jet energy. This reflects the three-body nature of the $\nu_4 \to \mu\bar{q}Q$ decay, and to a lesser degree the effect of the virtual W boson propagator. In the CELLO event, the two jets are less energetic than the two muons. Also, both jet masses are small, inhabiting the $m_{\text{jet}} \sim 0$–5-GeV region of Fig. 9(b). Thus the CELLO event is in an unfavored part of phase space, but more events of this type would be needed to rule out the $Z \to \nu_4\bar{\nu}_4$ interpretation.

IV. CONCLUSION

The decays of the Z^0 boson are a promising source of heavy fourth-generation charged leptons and neutrinos, provided their masses are less than $\frac{1}{2}M_Z$. The L signal at $p\bar{p}$ colliders is very low, but the signal of acollinear lepton pairs with $\not{p}_T$ would be distinctive. The production of L pairs at e^+e^- colliders operating on Z^0 resonance would be copious, and the various dilepton and lepton-plus-two-jet signals would be easily recognizable against standard-model backgrounds. Finally, the configuration of the CELLO μ–μ–two-jet event compares unfavorably with the $Z^0 \to \nu_4\bar{\nu}_4$ explanation, though more events are needed to make a definitive statement.

ACKNOWLEDGMENTS

One of us (H.B.) would like to thank Xerxes Tata for helpful discussions. This research was supported in part by the University of Wisconsin Research Committee with funds granted by the Wisconsin Alumni Research Foundation, and in part by the Department of Energy under Contract No. DE-AC02-76ER0881.

APPENDIX

In this appendix, we present the calculation of the cross section for pair production and decay of heavy leptons. The process considered is

$$q\bar{q} \to Z^0 \to L\bar{L}, \quad L \to \bar{\nu}_L + \bar{e}\nu_e, \quad L \to \nu_L + \bar{\nu}_\mu\mu \tag{A1}$$

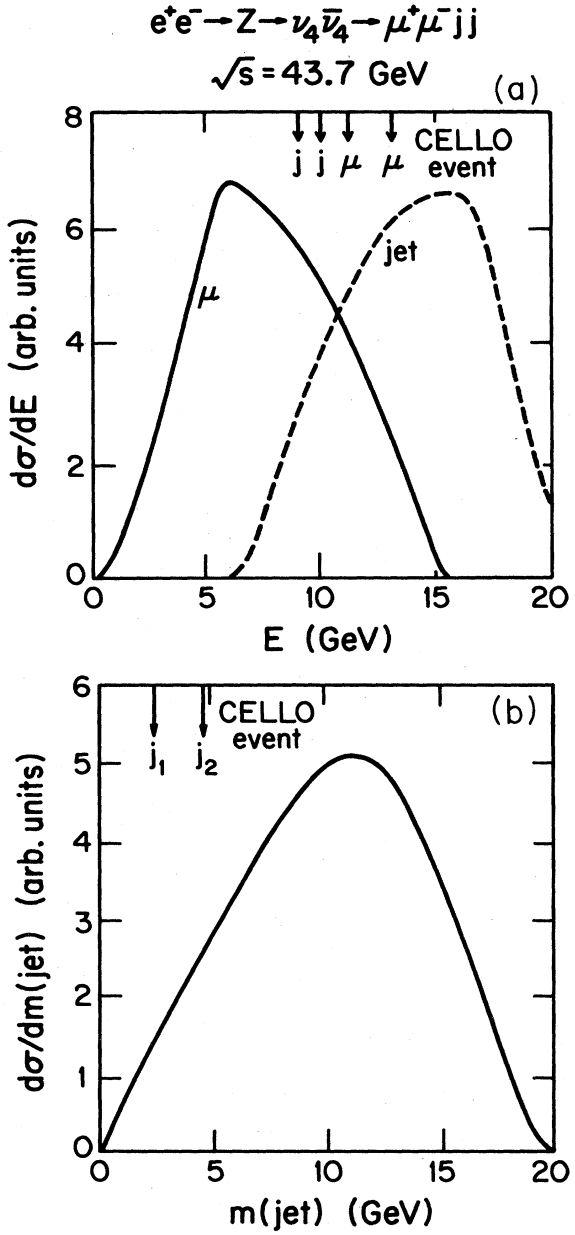

FIG. 9. Distributions in (a) lepton and jet energy and (b) jet invariant mass for the reaction $e^+e^- \to Z^0 \to \nu_4\bar{\nu}_4 \to l\bar{l} + 2$ jets at $\sqrt{s} = 43.4$ GeV. Also shown are the particle energies and jet masses of the $\mu\mu jj$ event observed by CELLO.

corresponding to the diagram in Fig. 4. It applies equally to $L \to \nu q\bar{q}'$ decays in one or both of L and $\bar{L}$, with appropriate substitutions.

The amplitude for this process is given by

$$\mathcal{M} = \frac{4G_F{}^3 M_W{}^4 M_Z{}^2}{\sqrt{2}} D_W(W_1{}^2) D_W(W_2{}^2) D_Z(\hat{s}) D_L(L^2) D_{\bar{L}}(\bar{L}^2) [\bar{u}(\nu_e)\gamma_\mu(1-\gamma_5)v(\bar{e})][\bar{u}(\mu)\gamma_\nu(1-\gamma_5)v(\bar{\nu}_\mu)]$$

$$\times \{\bar{v}(\bar{q})\gamma_\lambda[a_i(1-\gamma_5)+b_i(1+\gamma_5)]u(q)\}$$

$$\times \{\bar{u}(\nu_L)\gamma^\nu(1-\gamma_5)(\not{L}+m_L)\gamma^\lambda[a_f(1-\gamma_5)+b_f(1+\gamma_5)](\not{\bar{L}}-m_L)\gamma^\mu(1-\gamma_5)v(\bar{\nu}_L)\}\,, \tag{A2}$$

where

$$a=\frac{g_V+g_A}{2},\quad b=\frac{g_V-g_A}{2},$$

and particle labels are used to denote four-momenta. The squared matrix element is then

$$|\mathcal{M}|^2=|G|^2 8^3[\nu_e,\bar{e}]_{\mu\mu'}[\mu,\bar{\nu}_\mu]_{\nu\nu'}\{a_i{}^2[\bar{q},q]_{\lambda\lambda'}+b_i{}^2[q,\bar{q}]_{\lambda\lambda'}\}T^{\lambda\mu\nu\lambda'\mu'\nu'}, \tag{A3}$$

where we have defined

$$[x,y]_{\alpha\alpha'}=-x\cdot y\,g_{\alpha\alpha'}+x_\alpha y_{\alpha'}+x_{\alpha'}y_\alpha+i\epsilon_{\alpha\alpha'\beta\gamma}x^\beta y^\gamma, \tag{A4}$$

$$G=\frac{4G_F{}^3M_W{}^4M_Z{}^2}{\sqrt{2}}D_W(W_1{}^2)D_W(W_2{}^2)D_Z(\hat{s})D_L(L^2)D_{\bar{L}}(\bar{L}^2), \tag{A5}$$

and

$$T=\sum_{\text{spins}}|\bar{C}(\not{L}+m_L)A(\not{\bar{L}}-m_L)B|^2 \tag{A6}$$

with

$$\begin{aligned}&\bar{C}=\bar{u}(\nu_L)\gamma^\nu(1-\gamma_5),\\ &A=\gamma^\lambda[a_f(1-\gamma_5)+b_f(1+\gamma_5)],\\ &B=\gamma^\mu(1-\gamma_5)v(\bar{\nu}_L).\end{aligned} \tag{A7}$$

The evaluation of T can be broken up into smaller pieces using two Fierz transformations as in Ref. 9,

$$\begin{aligned}|\bar{C}(\not{L}+m)A(\not{\bar{L}}-m)B|^2=\tfrac{1}{4}\{&\mathrm{Tr}[(\not{L}+m)A(\not{\bar{L}}-m)\bar{A}][\bar{C}(\not{L}+m)C][\bar{B}(\not{\bar{L}}-m)B]\\ &+\eta^{\alpha\beta}\mathrm{Tr}[\gamma_5\gamma_\alpha(\not{L}+m)A(\not{\bar{L}}-m)\bar{A}][\bar{C}(\not{L}+m)\gamma_5\gamma_\beta C][\bar{B}(\not{\bar{L}}-m)B]\\ &+\eta'^{\rho\sigma}\mathrm{Tr}[(\not{L}+m)A\gamma_5\gamma_\rho(\not{\bar{L}}-m)\bar{A}][\bar{C}(\not{L}+m)C][\bar{B}(\not{\bar{L}}-m)\gamma_5\gamma_\sigma B]\\ &+\eta^{\alpha\beta}\eta'^{\rho\sigma}\mathrm{Tr}[\gamma_5\gamma_\alpha(\not{L}+m)A\gamma_5\gamma_\rho(\not{\bar{L}}-m)\bar{A}][\bar{C}(\not{L}+m)\gamma_5\gamma_\beta C][\bar{B}(\not{\bar{L}}-m)\gamma_5\gamma_\sigma B]\},\end{aligned} \tag{A8}$$

where

$$\eta^{\alpha\beta}=-g^{\alpha\beta}+\frac{L^\alpha L^\beta}{m^2},$$

$$\eta'^{\rho\sigma}=-g^{\rho\sigma}+\frac{\bar{L}^\rho\bar{L}^\sigma}{m^2},$$

and

$$\bar{A}=\gamma_0A^\dagger\gamma_0.$$

This expression is valid only for L and $\bar{L}$ on mass shell, which we assume. Evaluation of the traces in Eq. (A8) is lengthy but straightforward. We obtain

$$\begin{aligned}T=\tfrac{1}{4}8^3(&T_{11}^{\lambda\lambda'}T_{12}^{\nu\nu'}T_{13}^{\mu\mu'}+T_{21\alpha}^{\lambda\lambda'}T_{22}^{\nu\nu'\alpha}T_{23}^{\mu\mu'}\\ &+T_{31\rho}^{\lambda\lambda'}T_{32}^{\nu\nu'}T_{33}^{\mu\mu'\rho}+T_{41\alpha\rho}^{\lambda\lambda'}T_{42}^{\nu\nu'\alpha}T_{43}^{\mu\mu'\rho}),\end{aligned} \tag{A9}$$

where the tensors T_{ij} are

$$T_{11}^{\lambda\lambda'}=a_f{}^2[L,\bar{L}]^{\lambda\lambda'}+b_f{}^2[\bar{L},L]^{\lambda\lambda'}-2m_L{}^2a_fb_fg^{\lambda\lambda'}, \tag{A10a}$$

$$T_{12}^{\nu\nu'}=[\nu_L,L]^{\nu\nu'}, \tag{A10b}$$

$$T_{13}^{\mu\mu'}=[\bar{L},\bar{\nu}_L]^{\mu\mu'}, \tag{A10c}$$

$$\begin{aligned}T_{21\alpha}^{\lambda\lambda'}=m_L\{&-a_f{}^2[(\alpha),\bar{L}]^{\lambda\lambda'}+b_f{}^2[\bar{L},(\alpha)]^{\lambda\lambda'}\\ &+2a_fb_fi\epsilon^{\lambda\lambda'\gamma\alpha}L_\gamma\},\end{aligned} \tag{A10d}$$

$$T_{22}^{\nu\nu'\alpha}=\frac{1}{m_L}\{-L^\alpha[\nu_L,L]^{\nu\nu'}+m_L{}^2[\nu_L,(\alpha)]^{\nu\nu'}\}, \tag{A10e}$$

$$T_{23}^{\mu\mu'}=[\bar{L},\bar{\nu}_L]^{\mu\mu'}, \tag{A10f}$$

$$T_{31\rho}^{\lambda\lambda'}=m_L\{a_f{}^2[L,(\rho)]^{\lambda\lambda'}-b_f{}^2[(\rho),L]^{\lambda\lambda'}-2ia_fb_f\epsilon^{\lambda\lambda'\gamma}{}_\rho\bar{L}_\gamma\}, \tag{A10g}$$

$$T_{32}^{\nu\nu'}=[\nu_L,L]^{\nu\nu'}, \tag{A10h}$$

$$T_{33}^{\mu\mu'\rho}=-\frac{1}{m_L}\{-\bar{L}^\rho[\bar{L},\bar{\nu}_L]^{\mu\mu'}+m_L{}^2[(\rho),\bar{\nu}_L]^{\mu\mu'}, \tag{A10i}$$

$$\begin{aligned}T_{41\alpha\rho}^{\lambda\lambda'}=m_L{}^2\{&-a_f{}^2[(\alpha),(\rho)]^{\lambda\lambda'}-b_f{}^2[(\rho),(\alpha)]^{\lambda\lambda'}\}\\ &-2a_fb_ff_{\alpha\rho}^{\lambda\lambda'},\end{aligned} \tag{A10j}$$

$$T_{42}^{\nu\nu'\alpha}=\frac{1}{m_L}\{-L^\alpha[\nu_L,L]^{\nu\nu'}+m_L{}^2[\nu_L,(\alpha)]^{\nu\nu'}\}, \tag{A10k}$$

$$T_{43}^{\mu\mu'\rho}=-\frac{1}{m_L}\{-\bar{L}^\rho[\bar{L},\bar{\nu}_L]^{\mu\mu'}+m_L{}^2[(\rho),\bar{\nu}_L]^{\mu\mu'}\}, \tag{A10l}$$

and

$$\begin{aligned}f_{\alpha\rho}^{\lambda\lambda'}=&g_{\alpha\rho}(L^\lambda\bar{L}^{\lambda'}+L^{\lambda'}\bar{L}^\lambda)+g_\rho^\lambda(L_\alpha\bar{L}^{\lambda'}-\bar{L}_\alpha L^{\lambda'})\\ &-g_\rho^{\lambda'}(\bar{L}^\lambda L_\alpha+L^\lambda\bar{L}_\alpha)-g_\alpha^\lambda(L_\rho\bar{L}^{\lambda'}+L^{\lambda'}\bar{L}_\rho)\\ &-g_\alpha^{\lambda'}(L_\rho\bar{L}^\lambda-\bar{L}_\rho L^\lambda)+L\cdot\bar{L}(g_\alpha^\lambda g_\rho^{\lambda'}+g_\alpha^{\lambda'}g_\rho^\lambda)\\ &+g^{\lambda\lambda'}(L_\alpha\bar{L}_\rho+\bar{L}_\alpha L_\rho-L\cdot\bar{L}g_{\alpha\rho}).\end{aligned} \tag{A10m}$$

In the above expressions the notation is

$$[x,(\alpha)]^{\lambda\lambda'}y_\alpha=[x,y]^{\lambda\lambda'}\ . \tag{A11}$$

To obtain the final expression for the squared matrix element, we use the following contractions:

$$[w,x]_{\alpha\beta}[y,z]^{\alpha\beta}=4w\cdot y\,x\cdot z\ , \tag{A12a}$$

$$[x,y]_{\alpha\beta}g^{\alpha\beta}=-2x\cdot y\ , \tag{A12b}$$

$$i\epsilon^{\alpha\rho\lambda\lambda'}L_\rho[x,y]_{\lambda\lambda'}=2(x^\alpha y\cdot L-x\cdot L\,y^\alpha)\ . \tag{A12c}$$

The squared matrix element then reads

$$|\mathscr{M}|^2=|G|^2 8^6\frac{4^3}{4}(x_1+x_2+x_3+x_4) \tag{A13}$$

with

$$x_1=[(a_i^2a_f^2+b_i^2b_f^2)\bar{q}\cdot L\,q\cdot\bar{L}+(a_i^2b_f^2+b_i^2a_f^2)q\cdot L\,\bar{q}\cdot\bar{L}+(a_i^2+b_i^2)a_fb_fm_L^2q\cdot\bar{q}][\nu_e\cdot\bar{L}\,\bar{\nu}_L\cdot\bar{e}][\mu\cdot\nu_L\bar{\nu}_\mu\cdot L]\ , \tag{A14a}$$

$$\begin{aligned}x_2=&[(a_i^2b_f^2-b_i^2a_f^2)(-\bar{\nu}_\mu\cdot L\,q\cdot L+m_L^2q\cdot\bar{\nu}_\mu)\bar{q}\cdot\bar{L}+(b_i^2b_f^2-a_i^2a_f^2)(-\bar{\nu}_\mu\cdot L\,\bar{q}\cdot L+m_L^2\bar{q}\cdot\bar{\nu}_\mu)q\cdot\bar{L}\\&+(a_i^2-b_i^2)a_fb_fm_L^2(\bar{q}\cdot L\,q\cdot\bar{\nu}_\mu-q\cdot L\,\bar{q}\cdot\bar{\nu}_\mu)][\nu_e\cdot\bar{L}\bar{\nu}_L\cdot\bar{e}](\mu\cdot\nu_L)\ ,\end{aligned} \tag{A14b}$$

$$\begin{aligned}x_3=-&[(a_i^2b_f^2-b_i^2a_f^2)(\nu_e\cdot\bar{L}\,\bar{q}\cdot\bar{L}-m_L^2\bar{q}\cdot\nu_e)q\cdot L+(b_i^2b_f^2-a_i^2a_f^2)(\nu_e\cdot\bar{L}\,q\cdot\bar{L}-m_L^2q\cdot\nu_e)\bar{q}\cdot L\\&+(a_i^2-b_i^2)a_fb_fm_L^2(\bar{q}\cdot\bar{L}\,q\cdot\nu_e-q\cdot\bar{L}\,\bar{q}\cdot\nu_e)][\mu\cdot\nu_L\bar{\nu}_\mu\cdot L](\bar{\nu}_L\cdot\bar{e})\ ,\end{aligned} \tag{A14c}$$

$$\begin{aligned}x_4=(\bar{\nu}_L\cdot\bar{e})(\mu\cdot\nu_L)\{&(a_i^2a_f^2+b_i^2b_f^2)[\bar{q}\cdot L\,q\cdot\bar{L}\,\nu_e\cdot\bar{L}\,\bar{\nu}_\mu\cdot L-m_L^2(q\cdot\nu_e\bar{q}\cdot L\,\bar{\nu}_\mu\cdot L+q\cdot\bar{L}\,\bar{q}\cdot\bar{\nu}_\mu\nu_e\cdot\bar{L})+m_L^4q\cdot\nu_e\bar{q}\cdot\bar{\nu}_\mu]\\&+(a_i^2b_f^2+b_i^2a_f^2)[\bar{q}\cdot\bar{L}\,q\cdot L\,\nu_e\cdot\bar{L}\,\bar{\nu}_\mu\cdot L-m_L^2(\bar{q}\cdot\nu_eq\cdot L\,\bar{\nu}_\mu\cdot L+\bar{q}\cdot\bar{L}\,q\cdot\bar{\nu}_\mu\nu_e\cdot\bar{L})+m_L^4\bar{q}\cdot\nu_eq\cdot\bar{\nu}_\mu]\\&+(a_i^2+b_i^2)a_fb_fm_L^2[\nu_e\cdot\bar{\nu}_\mu(q\cdot L\,\bar{q}\cdot\bar{L}+\bar{q}\cdot L\,q\cdot\bar{L})+L\cdot\bar{L}(q\cdot\nu_e\bar{q}\cdot\bar{\nu}_\mu+\bar{q}\cdot\nu_eq\cdot\bar{\nu}_\mu)\\&\quad-\bar{\nu}_\mu\cdot\bar{L}(q\cdot\nu_e\bar{q}\cdot L+\bar{q}\cdot\nu_eq\cdot L)-\nu_e\cdot L(q\cdot\bar{\nu}_\mu\bar{q}\cdot\bar{L}+\bar{q}\cdot\bar{\nu}_\mu q\cdot\bar{L})\\&\quad-q\cdot\bar{q}(L\cdot\bar{L}\,\nu_e\cdot\bar{\nu}_\mu-\bar{\nu}_\mu\cdot\bar{L}\,\nu_e\cdot L)]\}\ ,\end{aligned} \tag{A14d}$$

and

$$|G|^2=8G_F^6M_W^8M_Z^4\,|D_W(W_1^2)|^2\,|D_W(W_2^2)|^2\,|D_Z(\hat{s})|^2\left[\frac{\pi}{m_L\Gamma_L}\right]^2\delta(L^2-m_L^2)\delta(\bar{L}^2-m_L^2)\ . \tag{A15}$$

The term x_1 is just the product of production and decay-squared matrix elements; it integrates to the total cross section. In the terms x_2 and x_3, one decay of L or $\bar{L}$ factorizes, while in the term x_4, there is no factorization of production and decay. The terms x_2, x_3, and x_4 each integrate to give no contribution to the total cross section.

Equation (A13) can be easily adapted to heavy-lepton production through a virtual photon by the following substitutions in Eq. (A15):

$$\begin{aligned}&32G_F^2M_Z^4\to e^4\ ,\\&g_V^{i,f}\to Q_{i,f}\ ,\\&g_A^{i,f}\to 0\ ,\\&|D_Z(\hat{s})|^2\to 1/\hat{s}^2\ ,\end{aligned} \tag{A16}$$

where $Q_{i,f}$ is the charge of the initial/final fermion in units of e.

[1]V. Barger, H. Baer, K. Hagiwara, and R. J. N. Phillips, Phys. Rev. D **30**, 947 (1984).
[2]V. Barger, H. Baer, A. D. Martin, E. W. N. Glover, and R. J. N. Phillips, Phys. Lett. **133B**, 449 (1983); Phys. Rev. D **29**, 2020 (1984).
[3]D. Cline and C. Rubbia, Phys. Lett. **127B**, 277 (1983).
[4]S. Gottlieb and T. Weiler, Phys. Rev. D **29**, 2005 (1984).
[5]V. Barger, W. Y. Keung, and R. J. N. Phillips, Phys. Lett. **141B**, 126 (1984).
[6]D. Dicus, S. Nandi, W. W. Repko, and X. Tata, Phys. Rev. D **29**, 67 (1984).
[7]R. Thun, Phys. Lett. **134B**, 459 (1984).
[8]M. Gronau, C. N. Leung, and J. L. Rosner, Phys. Rev. D **29**, 2539 (1984).
[9]T. Schimert, C. Burgess, and X. Tata, Phys. Rev. D **32**, 707 (1985).
[10]W. Bartel *et al.*, Phys. Lett. **123B**, 353 (1983); R. Brandelik *et al.*, *ibid.* **99B**, 163 (1981); C. H. Berger *et al.*, *ibid.* **99B**, 489 (1981); D. P. Barber *et al.*, Phys. Rev. Lett. **45**, 1904 (1980).
[11]H. J. Behrend *et al.*, Phys. Lett. **141B**, 145 (1984).
[12]J. L. Rosner, Nucl. Phys. **B248**, 503 (1984).
[13]H. Baer, J. Ellis, D. V. Nanopoulos, and X. Tata, Phys. Lett. **153B**, 265 (1985).
[14]D. Duke and J. F. Owens, Phys. Rev. D **30**, 49 (1984).